

# CAOS: Conformal Aggregation of One-Shot Predictors

Maja Waldron<sup>1</sup>

## Abstract

One-shot prediction enables rapid adaptation of pretrained foundation models to new tasks using only one labeled example, but lacks principled uncertainty quantification. While conformal prediction provides finite-sample coverage guarantees, standard split conformal methods are inefficient in the one-shot setting due to data splitting and reliance on a single predictor. We propose **Conformal Aggregation of One-Shot Predictors (CAOS)**, a conformal framework that adaptively aggregates multiple one-shot predictors and uses a leave-one-out calibration scheme to fully exploit scarce labeled data. Despite violating classical exchangeability assumptions, we prove that **CAOS** achieves valid marginal coverage using a monotonicity-based argument. Experiments on one-shot facial landmarking and RAFT text classification tasks show that **CAOS** produces substantially smaller prediction sets than split conformal baselines while maintaining reliable coverage.

## 1. Introduction

Large pretrained foundation models enable rapid adaptation to new tasks using only a handful of labeled examples, without task-specific fine-tuning (Brown et al., 2020; Bommasani, 2021; Radford et al., 2021; Siméoni et al., 2025). In both vision and language, such one-shot and few-shot prediction paradigms are particularly attractive in settings where labeled data are scarce or expensive to obtain.

In these settings, each labeled example can serve as a demonstration that induces a task-specific predictor for new inputs. When multiple labeled examples are available, this naturally gives rise to a *collection* of one-shot predictors rather than a single fixed model. The quality and relevance of these predictors may vary substantially across test inputs, making it unclear which prediction to trust and how to quantify uncertainty in a principled way.

<sup>1</sup>Department of Statistics, University of Wisconsin-Madison, USA. Correspondence to: Maja Waldron <maja.waldron@wisc.edu>.

A motivating example arises in medical facial analysis, where clinicians annotate a small number of images with task-specific facial landmarks for pre- and post-operative assessment. Modern vision foundation models can transfer landmark information from a single annotated image to a new image via patch similarity (Siméoni et al., 2025), yielding a collection of one-shot predictors whose usefulness varies across patients and poses.

Beyond point predictions, practical deployment in such settings requires reliable uncertainty quantification. Conformal prediction provides a principled framework for constructing prediction sets with finite-sample marginal coverage guarantees (Shafer & Vovk, 2008; Angelopoulos et al., 2024). Applied naively, a common approach is to equip each one-shot predictor with its own conformal prediction set using split conformal calibration. However, data splitting is statistically inefficient in the low-data regimes that motivate one-shot learning (Bashari et al., 2025), and selecting or aggregating predictors adaptively typically violates the assumptions required for conformal validity (Liang et al., 2024).

These challenges motivate the following question: *Can we aggregate the predictions of all one-shot predictors induced by the available labeled data in a manner that adapts to each test input, uses labeled data efficiently for calibration, and still yields valid conformal prediction sets?*

In this work, we answer this question in the affirmative by introducing **Conformal Aggregation of One-Shot Predictors (CAOS)**, a conformal framework for one-shot prediction. At a high level, **CAOS** adaptively aggregates nonconformity scores across multiple one-shot predictors while allowing all labeled examples to participate in calibration through a leave-one-out construction. Despite breaking classical exchangeability at the score level, **CAOS** achieves exact finite-sample marginal coverage guarantees.

Our contributions are threefold: (i) we introduce **CAOS**, a data-efficient conformal framework for aggregating one-shot predictors without requiring disjoint calibration splits; (ii) we establish exact finite-sample coverage guarantees for **CAOS** via a novel monotonicity-based reduction to full conformal prediction; and (iii) we demonstrate empirically that **CAOS** yields substantially smaller prediction sets than split conformal baselines while maintaining reliable coverage in both vision and language one-shot tasks.

## 2. Related Work

In-Context Learning (ICL), originally developed in language models (Brown et al., 2020), together with related zero-shot and few-shot prediction paradigms (Bommasani, 2021), has become a standard approach for adapting large pretrained models in both language and vision (Radford et al., 2021; Siméoni et al., 2025). Due to its distribution-free assumptions, conformal prediction (Angelopoulos et al., 2023; 2024) is an attractive framework for uncertainty quantification, as it allows pretrained models to be treated as black boxes while achieving marginal coverage guarantees.

Recent work has applied conformal prediction to large pretrained models in zero-shot, one-shot, and few-shot regimes (Fisch et al., 2021; Park et al., 2023; Fillioux et al., 2024; Quach et al., 2023; Su et al., 2024; Wang et al., 2024; Vishwakarma et al., 2024; Pantelidis et al., 2025; Ye & Wen, 2025; Lin et al., 2025; Tayebati et al., 2025; Silva-Rodríguez et al., 2025a,b; Wang et al., 2025; Xu & Lu, 2025), typically using split conformal calibration for simplicity. In one-shot settings, however, each labeled example induces a distinct predictor, giving rise to a collection of predictors rather than a single fixed model. Existing conformal approaches largely ignore this structure, leaving uncertainty quantification for collections of one-shot predictors underexplored.

While few-shot adaptation is particularly attractive when labeled data are scarce, this regime exacerbates a fundamental trade-off in classical conformal prediction. Split conformal is computationally efficient but statistically inefficient in low-data regimes (Bashari et al., 2025), while full conformal improves statistical efficiency at prohibitive computational cost. Cross-conformal prediction (Vovk, 2015) and related leave-one-out methods (Barber et al., 2021) reuse data more effectively, but typically incur slack in their coverage guarantees due to non-exchangeable scores (Gasparin & Ramdas, 2025), resulting in a tension between efficiency, tractability, and exact validity in the one-shot setting.

When faced with a collection of predictors, a natural response is to either select a single predictor (Liang et al., 2024; Bai & Jin, 2024; Hegazy et al., 2025) or to aggregate predictions across predictors (Gasparin & Ramdas, 2024b; Rivera et al., 2024; Alami et al., 2025). However, most such approaches rely on disjoint data splits or additional calibration data to preserve coverage guarantees, which in turn limits data efficiency in small-sample regimes.

This inefficiency is not incidental, but stems from a central requirement of classical conformal prediction: standard coverage guarantees rely on the exchangeability of conformity scores for the calibration and test examples (Shafer & Vovk, 2008; Angelopoulos et al., 2023; 2024). In settings such as distribution shift (Tibshirani et al., 2019; Barber et al., 2023) or online prediction (Gasparin & Ramdas, 2024a; Sale &

Ramdas, 2025), exchangeability is violated at the data level, and valid coverage is typically recovered only at the cost of unavoidable slack terms (Barber et al., 2023). In the one-shot setting considered here, non-exchangeability instead arises algorithmically: aggregation or adaptive selection of predictors based on the observed data breaks exchangeability at the score level, even when the underlying data remain exchangeable, precluding the direct application of classical conformal arguments.

In contrast to the approaches discussed above, **CAOS** directly addresses the setting that motivates one-shot conformal prediction: small labeled datasets that induce a collection of reference-conditioned predictors whose relevance varies across test inputs. **CAOS** performs instance-adaptive aggregation of one-shot predictors while allowing all labeled examples to participate in calibration through a leave-one-out construction, thereby avoiding the statistical inefficiencies of data splitting. Although this aggregation breaks exchangeability of the conformity scores, **CAOS** leverages a monotonicity property <sup>1</sup> of the aggregated score to recover a sharp  $1 - \alpha$  finite-sample marginal coverage guarantee via a reduction to full conformal prediction. In this way, **CAOS** resolves the recurring trade-offs between adaptivity, data efficiency, computational tractability, and exact validity that characterize prior selection- and aggregation-based conformal methods in the one-shot, low-data regime.

## 3. Background

We now formalize the one-shot prediction setting discussed above and introduce the notation used throughout the paper. The basic building blocks of our framework are one-shot predictors and their associated nonconformity scores, while split conformal calibration is reviewed as a reference point.

We assume access to a pool of  $n$  labeled examples  $\mathcal{D}_n = \{(X_i, Y_i)\}_{i=1}^n$ . Each example induces a *one-shot predictor* through a fixed prediction mechanism  $\pi$ , defined as

$$\pi_i(\cdot | x) := \pi(\cdot | x; (X_i, Y_i)). \quad (1)$$

Because the predictor  $\pi_i$  depends on the specific reference example  $(X_i, Y_i)$ , predictions for a single test input  $x$  may vary substantially across the  $n$  reference examples.

To assess how well a candidate label  $y$  conforms to a test input  $x$  under a one-shot predictor  $\pi_i$ , we associate each predictor with a *nonconformity score*

$$s_{\pi_i}(x, y) \in \mathbb{R}, \quad (2)$$

<sup>1</sup>Interestingly, the theoretical arguments of Jin & Candès (2023) also rely on the monotonicity of the conformity scores, albeit in a different setting (to establish FDR control in multiple selection as opposed to marginal coverage in conformal one-shot prediction) and a different type of monotonicity (monotonicity w.r.t. the labels as opposed to monotonicity w.r.t. a larger reference set).

where smaller values indicate more conforming predictions. This abstraction allows different one-shot prediction mechanisms to be treated uniformly within the conformal prediction framework. We next describe two concrete instantiations of one-shot prediction and their corresponding nonconformity scores that are used in our experiments.

**Example 1: Landmark Transfer by Patch Similarity.** We consider a landmark localization task in which each reference image is divided into  $K$  patches and labeled with  $Y_i \in \mathcal{Y} = \{1, \dots, K\}$  indicating which patch contains the landmark of interest. One-shot landmark transfer leverages the embedding space of a pretrained vision model (e.g., DinoV3 (Siméoni et al., 2025)) to predict the location of the landmark in a new image  $x$  based on patch similarity. Let  $e_x(y)$  denote the embedding of patch  $y$  in image  $x$ .

The nonconformity score induced by reference example  $(X_i, Y_i)$  is defined as

$$s_{\pi_i}(x, y) = 1 - \text{sim}(e_x(y), e_{X_i}(Y_i)), \quad (3)$$

where  $\text{sim}(\cdot, \cdot)$  denotes cosine similarity. A point prediction corresponds to the most conforming label,

$$\hat{y} = \arg \min_{y \in \mathcal{Y}} s_{\pi_i}(x, y). \quad (4)$$

**Example 2: One-Shot Text Classification with LLMs.**

We next consider text classification with a fixed label set  $\mathcal{Y}$  using a **Large Language Model (LLM)**. Given a labeled reference example  $(X_i, Y_i)$  and a test input  $x$ , we construct a prompt of the form

Given input  $X_i$ , the correct output is  $Y_i$ .  
Now for input  $x$ , the output is: (5)

(see Sec. D.3 for the full prompt template), which conditions the model on a single demonstration.

For each candidate label  $y \in \mathcal{Y}$ , we define the nonconformity score as the average negative log-likelihood of  $y$  under the model,

$$s_{\pi_i}(x, y) = \text{AvgNLL}(y \mid \text{prompt}(X_i, Y_i, x)), \quad (6)$$

where the negative log-likelihood is normalized by the token length of  $y$  to avoid penalizing longer labels. As in Eqn. (4), a point prediction is obtained by minimizing this score over  $y \in \mathcal{Y}$ . While **LLMs** can condition on multiple in-context examples, in the one-shot setting each reference example induces its own predictor  $\pi_i$ .

Large pretrained models may yield strong point predictions when used as one-shot predictors. However, there is no principled way to assess the reliability of these predictions for a new input. In the next section, we introduce split conformal one-shot prediction, which equips each one-shot

predictor  $\pi_i$  with a data-dependent prediction set that enjoys finite-sample marginal coverage guarantees.

**Split conformal one-shot prediction.** A natural approach to uncertainty quantification for one-shot predictors is split conformal prediction. Given labeled data split into a reference set  $\mathcal{D}_{\text{ref}}$  and a disjoint calibration set  $\mathcal{D}_{\text{cal}}$ , each reference example  $(X_i, Y_i) \in \mathcal{D}_{\text{ref}}$  induces a one-shot predictor  $\pi_i$ , which can be equipped with a conformal prediction set using calibration data.

For a fixed predictor  $\pi_i$ , calibration scores are obtained by evaluating the nonconformity score  $s_{\pi_i}(X_j, Y_j)$  on calibration examples  $(X_j, Y_j) \in \mathcal{D}_{\text{cal}}$ , yielding the score set

$$\mathcal{S}_{\text{split}}^i = \{s_{\pi_i}(X_j, Y_j) : (X_j, Y_j) \in \mathcal{D}_{\text{cal}}\}. \quad (7)$$

From this set, a split conformal threshold is computed as

$$\hat{q}_{\text{split}}^i = \text{Quantile}(\mathcal{S}_{\text{split}}^i ; (1 - \alpha)(1 + 1/|\mathcal{D}_{\text{cal}}|)), \quad (8)$$

leading to the prediction set

$$\hat{C}_{\text{split}}^i(X_{n+1}) = \{y \in \mathcal{Y} : s_{\pi_i}(X_{n+1}, y) \leq \hat{q}_{\text{split}}^i\}. \quad (9)$$

Under exchangeability of the calibration data and test point, each  $\hat{C}_{\text{split}}^i(X_{n+1})$  satisfies the marginal coverage guarantee

$$\mathbb{P}(Y_{n+1} \in \hat{C}_{\text{split}}^i(X_{n+1})) \geq 1 - \alpha. \quad (10)$$

Split conformal one-shot prediction yields a valid prediction set for each reference example, but the resulting sets vary widely in size and usefulness, reflecting heterogeneity in one-shot predictor quality. Ideally, predictions would adaptively select or combine the most relevant reference examples for each test input. This creates a basic tension in the one-shot setting: predictive performance benefits from reusing all labeled examples, while conformal calibration restricts such reuse. We resolve this tension with Conformal Aggregation of One-Shot Predictors (**CAOS**), a conformal framework that aggregates one-shot predictors while allowing all labeled examples to participate in calibration.

## 4. Method

**Problem setting and goal.** We consider a one-shot prediction setting with  $n$  labeled examples  $\mathcal{D}_n = \{(X_i, Y_i)\}_{i=1}^n$ . Each labeled example induces a one-shot predictor  $\pi_i$  with an associated nonconformity score  $s_{\pi_i}$ . Our goal is to construct prediction sets  $\hat{C}_{\text{caos}}(X_{n+1})$  that satisfy finite-sample marginal coverage guarantees while remaining as small as possible. Smaller prediction sets correspond to more informative predictions and reduced predictive uncertainty.

No single reference example is uniformly optimal: the informativeness of one-shot predictors varies substantially across

reference examples and may depend on the test input. The central challenge is therefore to design a method that (i) aggregates information across multiple one-shot predictors, (ii) calibrates the resulting aggregate using the same limited labeled data, and (iii) retains finite-sample coverage guarantees. We address this challenge with **CAOS**, a leave-one-out conformal aggregation strategy that leverages all labeled data for both aggregation and calibration.

**CAOS score aggregation.** For notational convenience, given a dataset  $\mathcal{D}$  and a target pair  $(x, y)$ , we define the multiset of one-shot nonconformity scores

$$\mathcal{A}_{\mathcal{D}}(x, y) := \{s_{\pi_j}(x, y) : (X_j, Y_j) \in \mathcal{D}\}. \quad (11)$$

That is,  $\mathcal{A}_{\mathcal{D}}(x, y)$  collects the nonconformity scores for  $(x, y)$  induced by all reference examples in  $\mathcal{D}$ .

A key observation in the one-shot setting is that only a subset of reference examples are informative for a given test input. For instance, in landmark transfer, reference images with locally similar appearance yield more meaningful patch-similarity scores. Aggregating all  $n$  one-shot predictors uniformly therefore dilutes useful information with noise.

To address this, **CAOS** aggregates scores by focusing on the  $k$  *most informative* reference examples. Given a multiset of scores  $\mathcal{A} = \{a_i\}_{i=1}^n$  and an integer  $k \geq 1$ , we define the operator that aggregates the  $k$  smallest values in  $\mathcal{A}$  as,

$$\Sigma_{\min}^k(\mathcal{A}) := \sum_{j=1}^k a_{(j)}, \quad (12)$$

where  $a_{(1)} \leq a_{(2)} \leq \dots \leq a_{(n)}$  are the ordered values in  $\mathcal{A}$ . We will use this operator to select the  $k$  reference examples that are most compatible with the candidate output  $y$ .

For a test input  $X_{n+1}$  and candidate output  $y$ , let  $\mathcal{A}_{\mathcal{D}_n}(X_{n+1}, y)$  denote the pool of all one-shot nonconformity scores induced by examples in  $\mathcal{D}_n$ . The **CAOS** aggregated nonconformity score is defined as

$$s_{\text{caos}}((X_{n+1}, y); \mathcal{D}_n) := \frac{1}{k} \Sigma_{\min}^k(\mathcal{A}_{\mathcal{D}_n}(X_{n+1}, y)), \quad (13)$$

where  $k$  is a small constant (we use  $k = 3$  in all experiments). This score is small when several reference examples strongly support the candidate output  $y$ , and large otherwise. We explicitly indicate the dependence on  $\mathcal{D}_n$ , since unlike split conformal prediction, **CAOS** does not maintain disjoint reference and calibration sets.

**CAOS calibration and prediction sets.** To obtain valid prediction sets, the aggregated **CAOS** nonconformity scores must be calibrated. We adopt a *leave-one-out* calibration strategy. Specifically, for each labeled example  $(X_i, Y_i) \in \mathcal{D}_n$ , the **CAOS** calibration score is computed

without using  $(X_i, Y_i)$  as a reference example. We therefore define the leave-one-out dataset  $\mathcal{D}_n^{-i} = \mathcal{D}_n \setminus (X_i, Y_i)$  and let  $\mathcal{A}_{\mathcal{D}_n^{-i}}(X_i, Y_i)$  denote the collection of one-shot nonconformity scores induced by all reference examples in  $\mathcal{D}_n^{-i}$ .

The **CAOS** nonconformity score is

$$S_{\text{caos}}^i := \frac{1}{k} \Sigma_{\min}^k(\mathcal{A}_{\mathcal{D}_n^{-i}}(X_i, Y_i)). \quad (14)$$

Collecting these scores over all  $i = 1, \dots, n$ , we compute the empirical quantile

$$\hat{q}_{\text{caos}} = \text{Quantile}(\{S_{\text{caos}}^i\}_{i=1}^n; (1 - \alpha)(1 + 1/n)), \quad (15)$$

which mirrors the finite-sample correction used in split conformal prediction.

The resulting **CAOS** prediction set for a new input  $X_{n+1}$  is

$$\hat{C}_{\text{caos}}(X_{n+1}) = \{y \in \mathcal{Y} : s_{\text{caos}}((X_{n+1}, y); \mathcal{D}_n) \leq \hat{q}_{\text{caos}}\}. \quad (16)$$

**CAOS' coverage guarantees.** The leave-one-out calibration procedure treats test points differently from calibration data and therefore breaks the classical exchangeability assumptions used in conformal prediction. To establish valid coverage guarantees, we make the following assumption.

**Assumption 4.1** (Self-score optimality). For any labeled example  $(X_i, Y_i)$  in any dataset  $\mathcal{D}_n$ , the one-shot nonconformity score induced by using  $(X_i, Y_i)$  as its own reference is minimal among all one-shot scores for that target, i.e.,

$$s_{\pi_i}(X_i, Y_i) \leq s_{\pi_j}(X_i, Y_i) \quad \text{for all } (X_j, Y_j) \in \mathcal{D}_n. \quad (17)$$

This assumption reflects the natural property that a labeled example is maximally informative about itself, which holds in common one-shot settings such as patch similarity.

**Theorem 4.2** (Finite-sample coverage of **CAOS**). *Assume that the labeled data  $\mathcal{D}_n$  and the test example  $(X_{n+1}, Y_{n+1})$  are exchangeable and that Assumption 4.1 holds. Then the **CAOS** prediction set defined in Eqn. (16) satisfies the finite-sample marginal coverage guarantee*

$$\Pr(Y_{n+1} \in \hat{C}_{\text{caos}}(X_{n+1})) \geq 1 - \alpha. \quad (18)$$

The proof is nontrivial because the **CAOS** nonconformity scores are not exchangeable. In Sec. 5, we establish Thrm. 4.2 via a reduction to a theoretical full conformal variant of **CAOS**.

## 5. Theory: Coverage Guarantees for CAOS

This Section establishes Thrm. 4.2. The proof proceeds via a reduction to a theoretical full conformal version of

**Algorithm 1** CAOS Prediction

- 1: **Input:** Labeled data  $\mathcal{D}_n = \{(X_i, Y_i)\}_{i=1}^n$ ; test input  $X_{n+1}$ ; target coverage level  $1 - \alpha$ ; integer  $k \geq 1$ ; one-shot nonconformity score  $s_{\pi_i}$ .
- 2: Compute aggregated calibration scores via Eqn. (14):  
 $S_{\text{caos}}^i \leftarrow s_{\text{caos}}((X_i, Y_i); \mathcal{D}_n^{-i})$  for  $i = 1, \dots, n$ .
- 3: Compute threshold via Eqn. (15):  
 $\hat{q}_{\text{caos}} \leftarrow \text{Quantile}(\{S_{\text{caos}}^i\}_{i=1}^n; (1 - \alpha)(1 + 1/n))$ .
- 4: Compute test scores for all  $y \in \mathcal{Y}$  via Eqn. (13):  
 $S_{n+1}^y \leftarrow s_{\text{caos}}((X_{n+1}, y); \mathcal{D}_n)$ .
- 5: **Return** calibrated CAOS prediction set via Eqn. (16):  
 $\hat{C}_{\text{caos}}(X_{n+1}) \leftarrow \{y \in \mathcal{Y} : S_{n+1}^y \leq \hat{q}_{\text{caos}}\}$ .

**CAOS.** The argument relies on two key observations: (i) a monotonicity property of the CAOS nonconformity score with respect to the reference dataset, and (ii) a set inclusion result showing that CAOS prediction sets contain those produced by full conformal prediction. Together, these imply that CAOS inherits the finite-sample marginal coverage guarantee of full conformal prediction, despite using a computationally cheaper scoring rule that does not yield exchangeable scores.

### 5.1. Theoretical Construction of Full CAOS

Full conformal prediction is a rigorous but impractical version of conformal prediction. Split conformal prediction as described in Sec. 3, is often preferred due to its computational efficiency, which requires the scores to be calibrated only once, whereas full conformal prediction requires calibrating the threshold for each test example for each possible prediction label separately.<sup>2</sup> However, the computational efficiency of split conformal comes at the cost of statistical efficiency: while full conformal (and CAOS) use all of the labeled examples for calibration, split conformal can only use a fraction, e.g.  $n/2$ .

In this section, we describe a full conformal version of CAOS. This algorithm will never be run in practice due to the large computational cost. It is only needed for the theory to establish a rigorous coverage guarantee for CAOS as presented in Sec. 4.

For a test example  $X_{n+1}$  and every potential label  $y$ , we define the augmented dataset  $\mathcal{D}_{n+1}^y = \mathcal{D}_n \cup \{(X_{n+1}, y)\}$  and the augmented set of one-shot scores  $\mathcal{A}_{\mathcal{D}_{n+1}^y}(X_i, Y_i) = \{s_{\pi_j}(X_i, Y_i) : (X_j, Y_j) \in \mathcal{D}_{n+1}^y\}$ . Note that  $\mathcal{A}_{\mathcal{D}_{n+1}^y}(X_i, Y_i)$  augments the leave-one-out pool  $\mathcal{A}_{\mathcal{D}_n^{-i}}(X_i, Y_i)$  with both the self-score  $s_{\pi_i}(X_i, Y_i)$  and the

<sup>2</sup>In classical machine learning settings the underlying predictive model needs to also be retrained as many times, but in the one-shot setting considered here, there is at least no training involved.

score induced by the hypothetical test pair  $(X_{n+1}, y)$ . That is,  $\mathcal{A}_{\mathcal{D}_{n+1}^y}(X_i, Y_i)$  contains all one-shot nonconformity scores for the target pair  $(X_i, Y_i)$  obtained from the augmented set of reference examples. As an alternative to Eqn. (14), we define the full CAOS nonconformity scores

$$\begin{aligned} \tilde{S}_{\text{full}}^i &= \tilde{s}_{\text{caos}}((X_{n+1}, y); \mathcal{D}_{n+1}^y) \\ &= \frac{1}{k} (\Sigma_{\min}^{k+1}(\mathcal{A}_{\mathcal{D}_{n+1}^y}(X_i, Y_i)) - s_{\pi_i}(X_i, Y_i)). \end{aligned} \quad (19)$$

This definition differs slightly from the leave-one-out score  $s_{\text{caos}}$  defined in Eqn. (14). However, it is deliberately chosen to i) establish exchangeability of full CAOS and ii) such that, under Assump. 4.1, the test-time nonconformity scores of CAOS and full CAOS coincide, i.e.,

$$\tilde{s}_{\text{caos}}((X_{n+1}, y); \mathcal{D}_{n+1}^y) = s_{\text{caos}}((X_{n+1}, y); \mathcal{D}_n). \quad (20)$$

This equivalence (proof in Sec. C.1) will play a key role in the set-inclusion argument used to establish coverage for CAOS. Based on the calibration scores  $\tilde{S}_{\text{full}}^i$ , full CAOS requires a separate threshold for each test input  $y$

$$\hat{q}_{\text{full}}^y = \text{Quantile}\left(\{\tilde{S}_{\text{full}}^i\}_{i=1}^n; (1 - \alpha)(1 + 1/n)\right), \quad (21)$$

to construct the full conformal prediction set

$$\hat{C}_{\text{full}}(X_{n+1}) = \{y : \tilde{s}_{\text{caos}}((X_{n+1}, y); \mathcal{D}_{n+1}^y) \leq \hat{q}_{\text{full}}^y\}. \quad (22)$$

To establish conformal validity, full conformal prediction requires the scores to be symmetric.

**Lemma 5.1** (Symmetry of  $\tilde{s}_{\text{caos}}$ ). *For any dataset  $\mathcal{D}$  and any permutation  $\sigma$  of its elements,*

$$\tilde{s}_{\text{caos}}((x, y); \mathcal{D}) = \tilde{s}_{\text{caos}}((x, y); \mathcal{D}_\sigma).$$

*That is,  $\tilde{s}_{\text{caos}}$  is symmetric in its dataset argument.*

*Proof.* Fix  $(x, y)$  and a dataset  $\mathcal{D}$ . Let  $\mathcal{A}_{\mathcal{D}}(x, y)$  denote the multiset of one-shot nonconformity scores obtained by using each element of  $\mathcal{D}$  as a reference example for the target  $(x, y)$ . Permuting the elements of  $\mathcal{D}$  does not change this multiset, hence  $\mathcal{A}_{\mathcal{D}}(x, y) = \mathcal{A}_{\mathcal{D}_\sigma}(x, y)$ .

The operator  $\Sigma_{\min}^{k+1}$  depends only on the multiset of its inputs and is therefore symmetric. Moreover, the subtracted term in Eqn. (19) corresponds to the one-shot score induced by the target example itself and is unaffected by permutations of the remaining elements of  $\mathcal{D}$ . It follows that  $\tilde{s}_{\text{caos}}((x, y); \mathcal{D}) = \tilde{s}_{\text{caos}}((x, y); \mathcal{D}_\sigma)$ .  $\square$

By Lemma 5.1 and standard full conformal arguments (Angelopoulos et al., 2024), the prediction set defined in Eqn. (22) achieves finite-sample marginal coverage guarantees at the target level. We prove next that these guarantees extend to CAOS.

## 5.2. Conformal Validity of CAOS

We now prove Thrm. 4.2 by comparing the two constructions of CAOS: the leave-one-out calibrated prediction set defined in Eqn. (16) and the theoretical full conformal construction defined in Eqn. (22). The proof leverages the conformal validity of full CAOS via two steps: (i) a monotonicity lemma showing that the CAOS nonconformity scores can only improve as the reference set grows, and (ii) a comparison lemma relating leave-one-out CAOS scores to their full conformal analogues. Together, these yield the set inclusion  $\hat{C}_{\text{full}}(X_{n+1}) \subseteq \hat{C}_{\text{caos}}(X_{n+1})$ , which implies coverage.

**Lemma 5.2** (Monotonicity of the CAOS score). *Fix a target pair  $(x, y)$  and an integer  $k \geq 1$ . Let  $\mathcal{D} \subseteq \mathcal{D}'$  be two reference datasets with  $|\mathcal{D}| \geq k$ . Then*

$$s_{\text{caos}}((x, y); \mathcal{D}') \leq s_{\text{caos}}((x, y); \mathcal{D}).$$

That is, the CAOS nonconformity score can only improve (decrease) as the reference set grows.

*Proof.* Let  $\mathcal{A} = \mathcal{A}_{\mathcal{D}}(x, y)$  and  $\mathcal{A}' = \mathcal{A}_{\mathcal{D}'}(x, y)$ . Since  $\mathcal{D} \subseteq \mathcal{D}'$ , the multiset  $\mathcal{A}'$  contains all scores in  $\mathcal{A}$ .

Let  $a_{(1)} \leq \dots \leq a_{(|\mathcal{A}|)}$  denote the ordered values of  $\mathcal{A}$  and let  $a'_{(1)} \leq \dots \leq a'_{(|\mathcal{A}'|)}$  denote the ordered values of  $\mathcal{A}'$ . For each  $j \leq k$  we have  $a'_{(j)} \leq a_{(j)}$ , because adding elements to a multiset cannot increase any of the first  $k$  order statistics. Therefore,

$$\Sigma_{\min}^k(\mathcal{A}') = \sum_{j=1}^k a'_{(j)} \leq \sum_{j=1}^k a_{(j)} = \Sigma_{\min}^k(\mathcal{A}).$$

Dividing by  $k$  yields  $s_{\text{caos}}((x, y); \mathcal{D}') \leq s_{\text{caos}}((x, y); \mathcal{D})$ , as claimed.  $\square$

We can now use this Lemma to compare the calibration scores of CAOS and full CAOS.

**Lemma 5.3** (Comparison of CAOS and full CAOS scores). *Fix a candidate label  $y \in \mathcal{Y}$  and the augmented dataset  $\mathcal{D}_{n+1}^y = \mathcal{D}_n \cup \{(X_{n+1}, y)\}$ . Then for all  $i = 1, \dots, n$ ,*

$$\tilde{s}_{\text{caos}}((X_i, Y_i); \mathcal{D}_{n+1}^y) \leq s_{\text{caos}}((X_i, Y_i); \mathcal{D}_n^{-i}). \quad (23)$$

*Proof.* By the same argument in App. C.1 that uses Assum. 4.1 (self-score optimality) to establish the equivalence of test time scores (Eqn. (20)), we have

$$\begin{aligned} \tilde{s}_{\text{caos}}((X_i, Y_i); \mathcal{D}_{n+1}^y) \\ = s_{\text{caos}}((X_i, Y_i); \mathcal{D}_n^{-i} \cup \{X_{n+1}, y\}). \end{aligned} \quad (24)$$

Since  $\mathcal{D}_n^{-i} \cup \{X_{n+1}, y\}$  contains  $\mathcal{D}_n^{-i}$ , the claimed inequality follows from the monotonicity lemma (Lemma 5.2).  $\square$

Via a sequence of lemmas, we have established that the nonconformity scores of CAOS and full CAOS match on test inputs, while the CAOS scores dominate full CAOS on calibration inputs. As a result, full CAOS calibration leads to potentially smaller thresholds, which means that the resulting prediction sets are tighter than the CAOS prediction sets. We formalize this in the next corollary.

**Corollary 5.4** (Set inclusion). *Let  $\hat{C}_{\text{full}}(X_{n+1})$  be the full conformal CAOS set defined in Eqn. (22), and let  $\hat{C}_{\text{caos}}(X_{n+1})$  be the CAOS set defined in Eqn. (16). Then for any test input  $X_{n+1}$ ,*

$$\hat{C}_{\text{full}}(X_{n+1}) \subseteq \hat{C}_{\text{caos}}(X_{n+1}). \quad (25)$$

*Proof.* Let  $y \in \hat{C}_{\text{full}}(X_{n+1})$ . By definition of the prediction set (Eqn. (22)),  $y \leq \hat{q}_{\text{full}}^y$ . By Lemma 5.3,  $\tilde{s}_{\text{caos}}((X_i, Y_i); \mathcal{D}_{n+1}^y) \leq s_{\text{caos}}((X_i, Y_i); \mathcal{D}_n^{-i})$  for all calibration indices  $i = 1, \dots, n$ . These calibration scores are used to establish  $\hat{q}_{\text{caos}}$  and  $\hat{q}_{\text{full}}^y$  via Eqns. (15) and (21) respectively. Since the quantile function  $\text{Quantile}(\cdot; (1 - \alpha)(1 + 1/n))$  is monotonic in its first argument, the resulting thresholds obey  $\hat{q}_{\text{full}}^y \leq \hat{q}_{\text{caos}}$ , which means that  $y \leq \hat{q}_{\text{caos}}$ . Therefore, by Eqn. (16),  $y \in \hat{C}_{\text{caos}}(X_{n+1})$ .  $\square$

*Proof of Thrm. 4.2.* By the symmetry of  $\tilde{s}_{\text{caos}}((x, y); \mathcal{D}_{n+1}^y)$  (Lemma 5.1) and the assumed exchangeability of samples from the augmented dataset  $\mathcal{D}_{n+1}^y$ , standard full conformal arguments (Angelopoulos et al., 2024) imply finite-sample marginal coverage:

$$\Pr(Y_{n+1} \in \hat{C}_{\text{full}}(X_{n+1})) \geq 1 - \alpha. \quad (26)$$

Next, by the set inclusion argument (Corr. 5.4), the event  $\{Y_{n+1} \in \hat{C}_{\text{full}}(X_{n+1})\}$  implies the event  $\{Y_{n+1} \in \hat{C}_{\text{caos}}(X_{n+1})\}$ , and hence

$$\Pr(Y_{n+1} \in \hat{C}_{\text{caos}}(X_{n+1})) \geq \Pr(Y_{n+1} \in \hat{C}_{\text{full}}(X_{n+1}))$$

Together with Eqn. (26), this establishes Thrm. 4.2.  $\square$

**Remarks.** The CAOS coverage guarantee applies to nonconformity scores that satisfy two structural properties: (i) symmetry with respect to permutations of the reference data, and (ii) monotonicity with respect to the inclusion of additional examples. Score functions that violate these conditions, such as scores involving parameters retrained on the augmented dataset, fall outside the scope of our theory.

Although CAOS deliberately breaks score exchangeability by excluding the test point from the reference data, this does not compromise coverage. The monotonicity property implies that CAOS prediction sets contain those produced by full conformal prediction, rendering score exchangeability unnecessary for marginal coverage guarantees.

## 6. Experiments

We evaluate **CAOS** as a method for producing calibrated prediction sets for one-shot prediction in comparison to several **Split Conformal One-shot Predictor (SCOS)** baselines, namely (i) exemplar-based facial landmarking with pretrained vision models, and (ii) **Real World Few-Shot Annotated Tasks (RAFT)** with **LLMs**.

### 6.1. Exemplar-Based Facial Landmarking

This application is motivated by an ongoing collaboration with pediatric surgeons, who manually annotate patient images pre- and post-operatively to support medical screening and quantitative analysis of surgical outcomes. These analyses rely on task-specific facial landmarks that are not available in standard landmarking datasets and must be defined and annotated by clinical experts.

While pretrained vision models provide a strong foundation for landmark detection, fully supervised fine-tuning is often impractical in this setting. Clinical annotations are expensive and time-consuming, and while hundreds of labeled examples may be feasible, large-scale annotation is rarely realistic. As a result, approaches that rely on extensive fine-tuning are typically out of reach.

Instead, each annotated image can be viewed as an exemplar that induces a one-shot predictor, for example by transferring landmarks via patch similarity in a pretrained embedding space. Aggregating such predictors provides a natural way to leverage limited labeled data without additional training. However, exemplar relevance varies substantially across target images, making uncertainty-aware adaptive aggregation essential for reliable deployment.

We evaluate **CAOS** in this regime using publicly available face data, enabling controlled evaluation while supporting reproducibility and dissemination of results.

**Facial Landmarking Dataset.** We evaluate exemplar-based facial landmarking using aligned face images from the CelebA dataset. For reproducibility, the exact hash of the dataset version we used along with other relevant implementation details is provided in Appendix D.1.

Each image is divided into  $K = 168$  patches of  $16 \times 16$  pixels. The label  $Y$  for image  $X$  indicates in which of the  $K$  patches a landmark is located in, i.e. we treat facial landmarking as a classification problem with 168 classes. Other than padding images on the lower right to the next multiple of the patch size, we employ no further preprocessing.

Ground truth landmark locations are obtained via the MediaPipe Face Landmarker with default settings<sup>3</sup>, which places

<sup>3</sup>num\_faces=1, min\_face\_detection\_confidence=0.5, min\_face\_detection\_confidence=0.5

478 landmarks in each image. This auto-annotation scheme provides a scalable way to generate labeled data for 478 landmarking tasks of varying difficulty. While we acknowledge that MediaPipe Face Landmarker could make mistakes, it nevertheless produces a meaningful benchmark for the evaluation of one-shot landmarking via patch similarity.

We randomly select a subset of images, excluding any images where MediaPipe Landmarker fails to place any of the 478 landmarks, to create separate splits  $\mathcal{D}_n$  and  $\mathcal{D}_{\text{test}}$  with  $|\mathcal{D}_n| = |\mathcal{D}_{\text{test}}| = 100$ . All conformal approaches are evaluated on the same held-out set  $\mathcal{D}_{\text{test}}$ . For all split conformal approaches we further split  $\mathcal{D}_n$  into a reference set and a calibration set with  $|\mathcal{D}_{\text{ref}}| = |\mathcal{D}_{\text{cal}}| = 50$ ,  $\mathcal{D}_{\text{ref}} \cup \mathcal{D}_{\text{cal}} = \mathcal{D}_n$ .

**One-Shot Landmark Prediction via Patch Similarity.** Given an example image  $X_i$  with a landmark located in patch  $Y_i$ , the one-shot task is to predict where that same landmark is located in a test image. We instantiate one-shot landmarking using the patch-similarity approach described in Example 1. The embeddings  $e_x(y)$  in Eqn. (3), come from a pretrained frozen DINOv3 model (ViT-B/16 pre-trained on LVD-1689M) which produces a patch token for each image patch. The register and CLS tokens are dropped.

**Approaches for Conformal One-Shot Landmarking.** Given a dataset of  $|\mathcal{D}_n|$  labeled examples, we can instantiate  $|\mathcal{D}_n|$  one-shot predictors. Rather than point predictions, we want to obtain conformal prediction sets at a target miscoverage level  $\alpha$ , which are guaranteed to contain the true label with finite-sample marginal probability at least  $1 - \alpha$ .

Our guiding research question is how to leverage the available data to combine the one-shot predictors (e.g. by selecting the best ones for a new test example) while also using the available data to calibrate the conformal prediction sets.

We evaluate **CAOS** in comparison to several split conformal baselines in terms of empirical coverage and prediction set size (Eqns. (32) and (33) in Appendix D.2). Empirical coverage should meet or exceed the target level  $1 - \alpha$ , while smaller prediction sets, corresponding to lower predictive uncertainty, are preferred. For a fair comparison, all methods use the same one-shot prediction tasks, backbone models, and data splits, differing only in how prediction sets are constructed and calibrated.

- **SCOS Avg.:** This baseline follows Alg. 2 to calibrate  $|\mathcal{D}_{\text{ref}}|$  one-shot predictors on calibration data  $\mathcal{D}_{\text{cal}}$ . Performance is reported on average over one-shot predictors.
- **SCOS Best:** This baseline considers the same pool of one-shot predictors and calibration procedure but then uses the calibration set to select the predictor that produces the smallest prediction sets (on average over calibration examples). This selection step, in theory breaks the coverage guarantees associated with split conformal approaches.
- **SCOS Oracle:** This oracle variant is also based on Alg. 2,

Table 1. Empirical coverage  $\widehat{\text{Cov}}$  and prediction set size averaged over landmarks (mean  $\pm$  SEM) for exemplar-based facial landmarking, averaged over 478 landmarking tasks, at target miscoverage levels  $\alpha \in \{0.05, 0.1, 0.2\}$ .

Method	$\alpha = 0.05$		$\alpha = 0.1$		$\alpha = 0.2$	
	$\widehat{\text{Cov}} (\geq 0.95)$	$\widehat{\text{Size}}$	$\widehat{\text{Cov}} (\geq 0.9)$	$\widehat{\text{Size}}$	$\widehat{\text{Cov}} (\geq 0.8)$	$\widehat{\text{Size}}$
SCOS Avg.	$0.976 \pm 0.001$	$36.07 \pm 0.94$	$0.930 \pm 0.001$	$21.04 \pm 0.50$	$0.842 \pm 0.001$	$13.41 \pm 0.35$
SCOS Best	$0.952 \pm 0.002$	$20.49 \pm 0.59$	$0.898 \pm 0.002$	$12.17 \pm 0.32$	$0.797 \pm 0.003$	$7.12 \pm 0.18$
CAOS [ours]	$0.953 \pm 0.001$	<b><math>15.96 \pm 0.58</math></b>	$0.905 \pm 0.002$	<b><math>9.68 \pm 0.30</math></b>	$0.808 \pm 0.002$	<b><math>5.70 \pm 0.16</math></b>
SCOS Oracle <sup>†</sup>	$1.000 \pm 0.000$	$16.66 \pm 0.58$	$1.000 \pm 0.000$	$7.98 \pm 0.27$	$1.000 \pm 0.000$	$4.29 \pm 0.13$

<sup>†</sup> Uses hindsight knowledge of the test label; included as a non-deployable reference.

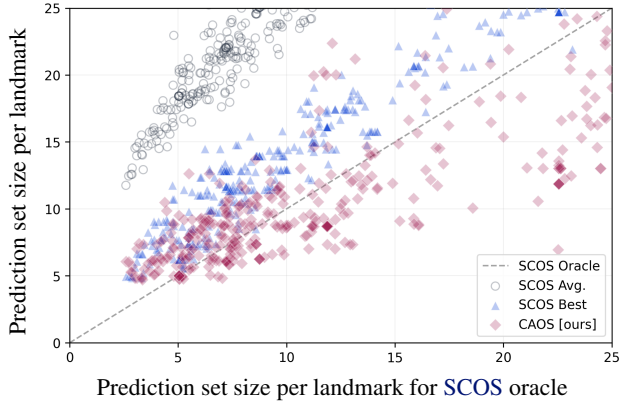


Figure 1. Prediction set size per landmark for exemplar-based facial landmarking. Each point corresponds to a landmark. CAOS yields smaller prediction sets than SCOS Avg. and SCOS Best, approaching oracle efficiency.

but leverages access to the test set and the ground-truth label to adaptively select, for each example, the smallest single-source prediction set that contains the true label. While this approach attains perfect coverage, it is not deployable in practice and is included solely as a reference.

- **CAOS [ours]:** Our approach uses  $\mathcal{D}_n$  both as the pool of reference examples and as calibration data according to Alg. 1. To avoid issues with hyperparameter selection we set the number of smallest scores to aggregate  $k = 3$  throughout.

**Results** Table 1 summarizes results in terms of empirical coverage and average set size at different target miscoverage rates  $\alpha \in [0.05, 0.1, 0.2]$ . We report mean and standard error around the mean averaged over the held-out test data and the 487 landmarking tasks. CAOS consistently meets or exceeds the target coverage rate, while significantly improving over the SCOS prediction sets in terms of size.

The scatter plot in Figure 1 further breaks down these results at  $\alpha = 0.05$  by individual landmarks which vary significantly by difficulty; on some landmarks even the oracle that selects the smallest prediction set that contains the true label achieves only prediction set sizes that exceed 20 patches



Figure 2. Conformal prediction set sizes for one-shot facial landmarking for SCOS (top) and CAOS (bottom) on three test images. Landmarks are colored by prediction set size. Smaller sets (green) correspond to lower predictive uncertainty and are preferable.

on average (averaged over held-out set). The x-axis is the prediction set size achieved by the SCOS oracle, while the values on the y-axis give the corresponding set size achieved by the other methods, SCOS Avg. (top) and CAOS (bottom) (the smaller the better, values below 10 are marked in green). We can see qualitatively that CAOS achieves significantly smaller prediction set sizes.

## 6.2. Real-World Few-Shot Annotated Tasks with LLMs

We evaluate CAOS on the RAFT benchmark, a collection of real-world few-shot text classification tasks designed to reflect practical annotation workflows. Each task provides a small labeled dataset and exhibits substantial heterogeneity in label space size, class balance, and semantic complexity, making RAFT a challenging testbed for uncertainty quantification in low-data regimes.

We treat each labeled example as inducing a one-shot predic-

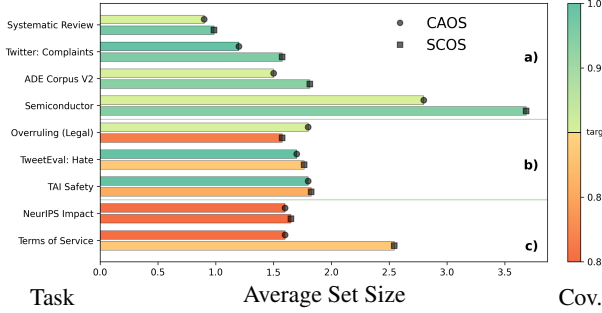


Figure 3. Comparison of **CAOS** (above) and **SCOS** (below) in terms of average prediction set size (x-axis, the smaller the better) and empirical coverage (color) for one-shot prediction with Llama2-7B on tasks from the RAFT dataset at  $\alpha = 0.1$ . **a)** For 4/9 tasks, both **CAOS** and **SCOS** hit target coverage. **b)** For 3/9 tasks only **CAOS** hits target coverage. **c)** For 2/9 tasks both miss. **CAOS** consistently achieves smaller prediction sets (in 8/9 tasks).

tor via **ICL** with a fixed prompt template. Given a reference example and a test input, a large language model produces a candidate label score without task-specific fine-tuning. This setup naturally yields a collection of one-shot predictors per task, whose quality varies across inputs and labels.

Our goal is to construct conformal prediction sets that adaptively aggregate these one-shot predictors while using the limited labeled data efficiently for calibration. We compare **CAOS** against split conformal one-shot baselines under identical backbones, prompts, and data splits, differing only in how prediction sets are calibrated and aggregated.

**One-shot Text Classification with LLMs.** We evaluate **CAOS** on one-shot text classification tasks from the RAFT benchmark, following the setup described in Sec. 3, Example 2, using a fixed prompt template (see Sec. D.3) and a frozen pretrained language model, specifically a 7B-parameter model from the Llama2 family.

Each **RAFT** task provides 50 labeled examples. We construct a dataset  $\mathcal{D}_n$  of size 40 and a held-out test set  $\mathcal{D}_{\text{test}}$  of size 10, which is used exclusively to evaluate empirical coverage and prediction set size. For split conformal baselines, which require disjoint reference and calibration data,  $\mathcal{D}_n$  is further partitioned into equally sized reference and calibration sets  $\mathcal{D}_{\text{ref}}$  and  $\mathcal{D}_{\text{calib}}$ . All methods use identical data splits, prompts, and backbone models, differing only in how prediction sets are constructed and calibrated.

For each candidate label  $y$  in the task-specific label space, we form a prompt by concatenating the reference example, the test input, and the candidate output. We compute the negative log-likelihood (NLL) of  $y$  under the model, and use the length-normalized NLL as the nonconformity score to avoid penalizing longer labels. While we use Llama2-7B in our experiments, this procedure applies to any language model that provides access to token-level logits, including

API-based models, provided the label space is known.

**Results.** Figure 3 summarizes the performance of **CAOS** and **SCOS** on one-shot text classification tasks from the RAFT benchmark using Llama2-7B at  $\alpha = 0.1$ . Across tasks, **CAOS** consistently produces smaller prediction sets than **SCOS**, achieving lower average set size in 8 out of 9 tasks. When both methods satisfy the target coverage level (4/9 tasks), **CAOS** maintains comparable coverage while yielding tighter prediction sets. In more challenging regimes, where **SCOS** fails to meet the target coverage, **CAOS** remains valid in 3 additional tasks. Only in 2 tasks do both methods fail to achieve the desired coverage.<sup>4</sup> These results indicate that **CAOS** improves efficiency without sacrificing reliability in the one-shot setting.

## 7. Conclusion

We introduced *Conformal Aggregation of One-Shot Predictors* (**CAOS**), a conformal prediction framework designed for one-shot and in-context learning settings where labeled data are scarce and multiple reference-induced predictors naturally arise. **CAOS** adaptively aggregates nonconformity scores across all available one-shot predictors while allowing every labeled example to participate in calibration.

Despite breaking classical exchangeability assumptions at the score level, we proved that **CAOS** achieves exact finite-sample marginal coverage. Our analysis relies on a novel monotonicity-based argument that reduces the **CAOS** procedure to full conformal prediction, thereby avoiding the slack terms that typically arise in cross-conformal or data-adaptive settings. This result shows that algorithmic departures from exchangeability need not preclude sharp coverage guarantees when carefully structured aggregation rules are used.

Empirically, we demonstrated that **CAOS** substantially improves efficiency over split conformal baselines in both vision and language applications, yielding significantly smaller prediction sets while maintaining reliable coverage. These gains are especially pronounced in low-data regimes, where data splitting and coarse calibration quantiles severely limit the usefulness of standard conformal approaches.

## Impact Statement

This paper presents work whose goal is to advance the field of Machine Learning. There are many potential societal consequences of our work, none of which we feel must be specifically highlighted here.

<sup>4</sup>Each **RAFT** task has a small evaluation set of size 10, which makes empirical coverage estimates inherently noisy. At a target coverage level of  $1 - \alpha = 0.9$ , even a perfectly calibrated method may observe only 8 out of 10 test examples covered in a given split. Accordingly, occasional deviations from the target coverage should be expected in this low-sample regime.

## References

Alami, N., Zakharia, J., and Taieb, S. B. Symmetric aggregation of conformity scores for efficient uncertainty sets. *arXiv preprint arXiv:2512.06945*, 2025.

Angelopoulos, A. N., Bates, S., et al. Conformal prediction: A gentle introduction. *Foundations and trends® in machine learning*, 16(4):494–591, 2023.

Angelopoulos, A. N., Barber, R. F., and Bates, S. Theoretical foundations of conformal prediction. *arXiv preprint arXiv:2411.11824*, 2024.

Bai, T. and Jin, Y. Optimized conformal selection: Powerful selective inference after conformity score optimization. *arXiv preprint arXiv:2411.17983*, 2024.

Barber, R. F., Candes, E. J., Ramdas, A., and Tibshirani, R. J. Predictive inference with the jackknife+. *The Annals of Statistics*, 49(1):486–507, 2021.

Barber, R. F., Candes, E. J., Ramdas, A., and Tibshirani, R. J. Conformal prediction beyond exchangeability. *The Annals of Statistics*, 51(2):816–845, 2023.

Bashari, M., Lotan, R. M., Lee, Y., Dobriban, E., and Romeno, Y. Synthetic-powered predictive inference. *arXiv preprint arXiv:2505.13432*, 2025.

Bommasani, R. On the opportunities and risks of foundation models. *arXiv preprint arXiv:2108.07258*, 2021.

Brown, T., Mann, B., Ryder, N., Subbiah, M., Kaplan, J. D., Dhariwal, P., Neelakantan, A., Shyam, P., Sastry, G., Askell, A., et al. Language models are few-shot learners. *Advances in neural information processing systems*, 33: 1877–1901, 2020.

Fillioux, L., Silva-Rodríguez, J., Ayed, I. B., Courne, P.-H., Vakalopoulou, M., Christodoulidis, S., and Dolz, J. Are foundation models for computer vision good conformal predictors? *arXiv preprint arXiv:2412.06082*, 2024.

Fisch, A., Schuster, T., Jaakkola, T., and Barzilay, R. Few-shot conformal prediction with auxiliary tasks. In *International Conference on Machine Learning*, pp. 3329–3339. PMLR, 2021.

Gasparin, M. and Ramdas, A. Conformal online model aggregation. *arXiv preprint arXiv:2403.15527*, 2024a.

Gasparin, M. and Ramdas, A. Merging uncertainty sets via majority vote. *arXiv preprint arXiv:2401.09379*, 2024b.

Gasparin, M. and Ramdas, A. Improving the statistical efficiency of cross-conformal prediction. *arXiv preprint arXiv:2503.01495*, 2025.

Hegazy, M., Aolaritei, L., Jordan, M. I., and Dieuleveut, A. Valid selection among conformal sets. *arXiv preprint arXiv:2506.20173*, 2025.

Jin, Y. and Candès, E. J. Selection by prediction with conformal p-values. *Journal of Machine Learning Research*, 24(244):1–41, 2023.

Liang, R., Zhu, W., and Barber, R. F. Conformal prediction after efficiency-oriented model selection. *arXiv preprint arXiv:2408.07066*, 2024.

Lin, Z., Li, Y., Sarna, N., Gao, Y., and von Gablenz, M. Domain-shift-aware conformal prediction for large language models. *arXiv preprint arXiv:2510.05566*, 2025.

Pantelidis, I., Rndl, K., and Henriksson, A. Efficient text classification with conformal in-context learning. *arXiv preprint arXiv:2512.05732*, 2025.

Park, S., Cohen, K. M., and Simeone, O. Few-shot calibration of set predictors via meta-learned cross-validation-based conformal prediction. *IEEE Transactions on Pattern Analysis and Machine Intelligence*, 46(1):280–291, 2023.

Quach, V., Fisch, A., Schuster, T., Yala, A., Sohn, J. H., Jaakkola, T. S., and Barzilay, R. Conformal language modeling. *arXiv preprint arXiv:2306.10193*, 2023.

Radford, A., Kim, J. W., Hallacy, C., Ramesh, A., Goh, G., Agarwal, S., Sastry, G., Askell, A., Mishkin, P., Clark, J., et al. Learning transferable visual models from natural language supervision. In *International conference on machine learning*, pp. 8748–8763. PMLR, 2021.

Rivera, E. O., Patel, Y., and Tewari, A. Conformal prediction for ensembles: Improving efficiency via score-based aggregation. *arXiv preprint arXiv:2405.16246*, 2024.

Sale, Y. and Ramdas, A. Online selective conformal inference: Errors and solutions. *Transactions on Machine Learning Research*, 2025.

Shafer, G. and Vovk, V. A tutorial on conformal prediction. *Journal of Machine Learning Research*, 9(3), 2008.

Silva-Rodríguez, J., Ben Ayed, I., and Dolz, J. Conformal prediction for zero-shot models. In *Proceedings of the Computer Vision and Pattern Recognition Conference*, pp. 19931–19941, 2025a.

Silva-Rodríguez, J., Ben Ayed, I., and Dolz, J. Trustworthy few-shot transfer of medical vlms through split conformal prediction. In *International Conference on Medical Image Computing and Computer-Assisted Intervention*, pp. 658–668. Springer, 2025b.

Siméoni, O., Vo, H. V., Seitzer, M., Baldassarre, F., Oquab, M., Jose, C., Khalidov, V., Szafraniec, M., Yi, S., Ramamonjisoa, M., et al. Dinov3. *arXiv preprint arXiv:2508.10104*, 2025.

Su, J., Luo, J., Wang, H., and Cheng, L. Api is enough: Conformal prediction for large language models without logit-access. *arXiv preprint arXiv:2403.01216*, 2024.

Tayebati, S., Kumar, D., Darabi, N., Jayasuriya, D., Krishnan, R., and Trivedi, A. R. Learning conformal abstention policies for adaptive risk management in large language and vision-language models. *arXiv preprint arXiv:2502.06884*, 2025.

Tibshirani, R. J., Foygel Barber, R., Candes, E., and Ramdas, A. Conformal prediction under covariate shift. *Advances in neural information processing systems*, 32, 2019.

Vishwakarma, H., Mishler, A., Cook, T., Dalmasso, N., Raman, N., and Ganesh, S. Prune'n predict: Optimizing llm decision-making with conformal prediction. *arXiv preprint arXiv:2501.00555*, 2024.

Vovk, V. Cross-conformal predictors. *Annals of Mathematics and Artificial Intelligence*, 74(1):9–28, 2015.

Wang, Z., Duan, J., Cheng, L., Zhang, Y., Wang, Q., Shi, X., Xu, K., Shen, H. T., and Zhu, X. Conu: Conformal uncertainty in large language models with correctness coverage guarantees. In *Findings of the Association for Computational Linguistics: EMNLP 2024*, pp. 6886–6898, 2024.

Wang, Z., Wang, Q., Zhang, Y., Chen, T., Zhu, X., Shi, X., and Xu, K. Sconu: Selective conformal uncertainty in large language models. *arXiv preprint arXiv:2504.14154*, 2025.

Xu, B. and Lu, Y. Tecp: Token-entropy conformal prediction for llms. *Mathematics*, 13(20):3351, 2025.

Ye, Y. and Wen, W. Data-driven calibration of prediction sets in large vision-language models based on inductive conformal prediction. *arXiv preprint arXiv:2504.17671*, 2025.

## A. Notation Summary

This appendix summarizes the notation used throughout the paper.

### Data and indices.

- $\mathcal{X}$ : input space.
- $\mathcal{Y}$ : output (label) space.
- $\mathcal{D}_n = \{(X_i, Y_i)\}_{i=1}^n$ : labeled reference dataset.
- $(X_{n+1}, Y_{n+1})$ : test example with ground truth label  $Y_{n+1}$ .
- $\mathcal{D}_n^{-i} = \mathcal{D}_n \setminus \{(X_i, Y_i)\}$ : leave-one-out dataset for index  $i$ .
- $\mathcal{D}_{n+1}^y = \mathcal{D}_n \cup \{(X_{n+1}, y)\}$ : dataset augmented with a hypothetical test label  $y$ .
- $i, j$ : indices of reference examples.
- $y \in \mathcal{Y}$ : candidate output label.

### One-shot predictors and nonconformity scores.

- $\pi_i(\cdot | x)$ : one-shot predictor induced by reference example  $(X_i, Y_i)$ .
- $s_{\pi_i}(x, y) = -\pi_i(y | x)$ : one-shot nonconformity score for target  $(x, y)$  using predictor  $\pi_i$ .
- $\mathcal{A}_{\mathcal{D}}(x, y) = \{s_{\pi_j}(x, y) : (X_j, Y_j) \in \mathcal{D}\}$ : pool of one-shot nonconformity scores for target  $(x, y)$  based on one-shot predictors induced by examples in  $\mathcal{D}$ . All score pools are interpreted as multisets.

### Aggregation and Quantile operators.

- $\Sigma_{\min}^k(\mathcal{A})$ : sum of the  $k$  smallest elements of multiset  $\mathcal{A}$ .
- Quantile( $\mathcal{S} ; \tau$ ): the  $\lceil \tau(|\mathcal{S}| + 1) \rceil$ -th order statistic of the multiset  $\mathcal{S}$ , for  $\tau \in (0, 1)$ .  
This definition accounts for ties and ensures finite-sample validity.
- The aggregation and quantile operators depend only on the multiset of values and are permutation invariant.

### Split conformal, CAOS, and full CAOS nonconformity scores.

- Test-time scores
  - $s_{\pi_i}(X_{n+1}, y)$ : split conformal one-shot nonconformity score induced by reference example  $i$ .
  - $s_{\text{caos}}((X_{n+1}, y) ; \mathcal{D}_n) = \frac{1}{k} \Sigma_{\min}^k(\mathcal{A}_{\mathcal{D}_n}(X_{n+1}, y))$ : CAOS test-time aggregated nonconformity score.
  - $\tilde{s}_{\text{caos}}((X_{n+1}, y) ; \mathcal{D}_{n+1}^y) = \frac{1}{k} (\Sigma_{\min}^{k+1}(\mathcal{A}_{\mathcal{D}_{n+1}^y}(X_i, Y_i)) - s_{\pi_i}(X_i, Y_i))$ : full CAOS test-time nonconformity score.
- Calibration scores
  - $s_{\pi_i}(X_j, Y_j)$ : split conformal calibration score for example  $j$  based on one-shot predictor  $\pi_i$ .
  - $s_{\text{caos}}((X_i, Y_i) ; \mathcal{D}_n^{-i}) = s_{\text{caos}}((X_i, Y_i) ; \mathcal{D}_n^{-i})$ : leave-one-out CAOS calibration score for example  $i$ .
  - $\tilde{s}_{\text{caos}}((X_i, Y_i) ; \mathcal{D}_{n+1}^y) = \tilde{s}_{\text{caos}}((X_i, Y_i) ; \mathcal{D}_{n+1}^y)$ : full CAOS calibration score for example  $i$ .
- Relationships between nonconformity scores
  - $\tilde{s}_{\text{caos}}((X_{n+1}, y) ; \mathcal{D}_{n+1}^y) = s_{\text{caos}}((X_{n+1}, y) ; \mathcal{D}_n)$ : test-time score equivalence between CAOS and full CAOS under Assumption 4.1.
  - $\tilde{s}_{\text{caos}}((X_i, Y_i) ; \mathcal{D}_{n+1}^y) \leq s_{\text{caos}}((X_i, Y_i) ; \mathcal{D}_n^{-i})$ : full CAOS calibration scores dominate CAOS.

Quantiles and prediction sets.

- $\hat{q}_{\text{split}}^i$ : split conformal threshold for one-shot predictor  $\pi_i$ .
- $\hat{q}_{\text{caos}}$ : CAOS calibration threshold.
- $\hat{q}_{\text{full}}^y$ : full CAOS calibration threshold.
- $\hat{C}_{\text{split}}^i(X_{n+1})$ : split conformal one-shot prediction set for predictor  $\pi_i$
- $\hat{C}_{\text{caos}}(X_{n+1})$ : CAOS prediction set.
- $\hat{C}_{\text{full}}(X_{n+1})$ : full conformal CAOS prediction set.

## B. Pseudocode

### Algorithm 2 Split Conformal One-Shot Prediction

- 1: **Input:** Example  $(X_i, Y_i)$  defining one-shot predictor  $i$ ; calibration set  $\mathcal{D}_{\text{cal}}$  of size  $|\mathcal{D}_{\text{cal}}|$ ; test point  $X_{n+1}$ ; target coverage level  $1 - \alpha$ ; nonconformity score  $s_{\pi_i}$ .
- 2: Compute set of calibration scores via Eqn. (7):  

$$\mathcal{S}_{\text{split}}^i \leftarrow \left\{ s_{\pi_i}(X_j, Y_j) : (X_j, Y_j) \in \mathcal{D}_{\text{cal}} \right\}.$$
- 3: Compute threshold via Eqn. (8):  

$$\hat{q}_{\text{split}}^i \leftarrow \text{Quantile}\left(\mathcal{S}_{\text{split}}^i ; (1 - \alpha)(1 + 1/|\mathcal{D}_{\text{cal}}|)\right).$$
- 4: **Return** prediction set via Eqn. (9):  

$$\hat{C}_{\text{split}}^i(X_{n+1}) \leftarrow \left\{ y \in \mathcal{Y} : s_{\pi_i}(X_{n+1}, y) \leq \hat{q}_{\text{split}}^i \right\}.$$

### Algorithm 3 CAOS Prediction (repeat of Alg. 1)

- 1: **Input:** Labeled data  $\mathcal{D}_n = \{(X_i, Y_i)\}_{i=1}^n$ ; test input  $X_{n+1}$ ; target coverage level  $1 - \alpha$ ; integer  $k \geq 1$ ; one-shot nonconformity score  $s_{\pi_i}$ .
- 2: Compute aggregated calibration scores via Eqn. (14):  

$$S_{\text{caos}}^i \leftarrow s_{\text{caos}}((X_i, Y_i); \mathcal{D}_n^{-i}) \text{ for } i = 1, \dots, n.$$
- 3: Compute threshold via Eqn. (15):  

$$\hat{q}_{\text{caos}} \leftarrow \text{Quantile}\left(\{S_{\text{caos}}^i\}_{i=1}^n ; (1 - \alpha)(1 + 1/n)\right).$$
- 4: Compute test scores for all  $y \in \mathcal{Y}$  via Eqn. (13):  

$$S_{n+1}^y \leftarrow s_{\text{caos}}((X_{n+1}, y); \mathcal{D}_n).$$
- 5: **Return** calibrated CAOS prediction set via Eqn. (16):  

$$\hat{C}_{\text{caos}}(X_{n+1}) \leftarrow \{y \in \mathcal{Y} : S_{n+1}^y \leq \hat{q}_{\text{caos}}\}.$$

## C. Detailed Proofs for CAOS Theory

### C.1. Proof of Test-Time Score Equivalence

We prove the identity

$$\tilde{s}_{\text{caos}}((X_{n+1}, y); \mathcal{D}_{n+1}^y) = s_{\text{caos}}((X_{n+1}, y); \mathcal{D}_n), \quad (27)$$

which is used in the set-inclusion argument in Sec. 5.

Recall that the CAOS test-time nonconformity score is defined as

$$s_{\text{caos}}((X_{n+1}, y); \mathcal{D}_n) = \frac{1}{k} \Sigma_{\min}^k(\{s_{\pi_i}(X_{n+1}, y) : (X_i, Y_i) \in \mathcal{D}_n\}). \quad (28)$$

**Algorithm 4** Full CAOS Prediction (Theoretical)

---

- 1: **Input:** Labeled data  $\mathcal{D}_n = \{(X_i, Y_i)\}_{i=1}^n$ ; test input  $X_{n+1}$ ; target coverage level  $1 - \alpha$ ; integer  $k \geq 1$ ; one-shot nonconformity score  $s_{\pi_i}(\cdot, \cdot)$ .
- 2: **for** each  $y \in \mathcal{Y}$  **do**
- 3:   Compute full CAOS calibration scores via Eqn. (19):  
 $\tilde{S}_{\text{full}}^i \leftarrow \tilde{s}_{\text{caos}}((X_i, Y_i); \mathcal{D}_{n+1}^y)$  for  $i = 1, \dots, n$ .
- 4:   Compute test score via Eqns. (13) and (20):  
 $S_{n+1}^y \leftarrow \tilde{s}_{\text{caos}}((X_{n+1}, y); \mathcal{D}_{n+1}^y)$
- 5:   Compute full conformal threshold via Eqn. (21):  
 $\hat{q}_{\text{full}}^y \leftarrow \text{Quantile}\left(\{\tilde{S}_{\text{full}}^i\}_{i=1}^n; (1 - \alpha)(1 + 1/n)\right)$ .
- 6: **end for**
- 7: **Return** full CAOS prediction set via Eqn. (22):  
 $\hat{\mathcal{C}}_{\text{full}}(X_{n+1}) \leftarrow \{y \in \mathcal{Y} : S_{n+1}^y \leq \hat{q}_{\text{full}}^y\}$ .

---

For full CAOS, the augmented dataset is  $\mathcal{D}_{n+1}^y = \mathcal{D}_n \cup \{(X_{n+1}, y)\}$ , and the corresponding test time score is

$$\tilde{s}_{\text{caos}}((X_{n+1}, y); \mathcal{D}_{n+1}^y) = \frac{1}{k} \left( \sum_{i=1}^{k+1} (\mathcal{A}_{\mathcal{D}_{n+1}^y}(X_{n+1}, y)) - s_{\pi_{n+1}}(X_{n+1}, y) \right), \quad (29)$$

where  $\mathcal{A}_{\mathcal{D}_{n+1}^y}(X_{n+1}, y)$  denotes the multiset of one-shot nonconformity scores obtained by using each element of  $\mathcal{D}_{n+1}^y$  as a reference for the target  $(X_{n+1}, y)$ .

By construction,

$$\mathcal{A}_{\mathcal{D}_{n+1}^y}(X_{n+1}, y) = \{s_{\pi_i}(X_{n+1}, y) : (X_i, Y_i) \in \mathcal{D}_n\} \cup \{s_{\pi_{n+1}}(X_{n+1}, y)\}. \quad (30)$$

Under Assump. 4.1, the self-score  $s_{\pi_{n+1}}(X_{n+1}, y)$  is minimal among all one-shot scores for the target  $(X_{n+1}, y)$ . Consequently, it is always included among the  $(k + 1)$  smallest elements of  $\mathcal{A}_{\mathcal{D}_{n+1}^y}(X_{n+1}, y)$ .

Subtracting this self-score therefore removes exactly one of the selected  $(k + 1)$  terms, leaving the sum of the  $k$  smallest scores induced by  $\mathcal{D}_n$ . Dividing by  $k$  yields

$$\tilde{s}_{\text{caos}}((X_{n+1}, y); \mathcal{D}_{n+1}^y) = \frac{1}{k} \sum_{i=1}^k (\{s_{\pi_i}(X_{n+1}, y) : (X_i, Y_i) \in \mathcal{D}_n\}), \quad (31)$$

which is precisely  $s_{\text{caos}}((X_{n+1}, y); \mathcal{D}_n)$ .  $\square$

## D. Additional Implementation Details

### D.1. Facial Landmarking Data

We use the Hugging Face dataset nielsr/CelebA-faces (aligned face crops of CelebA), train split (202,599 images; revision db26feecbaed40316ee4c80ec0e72211a2f4af6), with original resolution 178×218 and no additional resizing.

### D.2. Evaluation Metrics

All conformal prediction methods are evaluated in terms of empirical coverage and average prediction set size.

**Coverage.** Marginal coverage reports the fraction of prediction sets that contain the true label for labeled examples in the test set  $\mathcal{D}_{\text{test}}$ . We estimate empirical coverage as

$$\widehat{\text{Cov}} = \frac{1}{|\mathcal{D}_{\text{test}}|} \sum_{(X, Y) \in \mathcal{D}_{\text{test}}} \mathbb{1}\{Y \in \hat{\mathcal{C}}(X)\}, \quad (32)$$

reported either averaged per-task, or averaged jointly over all tasks. Eventhough SCOS and CAOS enjoy finite-sample marginal coverage guarantees, it can still occur that individual results lie below the target coverage of  $1 - \alpha$ . This is particularly prone to happen for small test sets  $\mathcal{D}_{\text{test}}$ .

**Set size.** We report the average prediction set size

$$\widehat{\text{Size}} = \frac{1}{|\mathcal{D}_{\text{test}}|} \sum_{(X, Y) \in \mathcal{D}_{\text{test}}} |\hat{\mathcal{C}}(X)|. \quad (33)$$

For the same marginal coverage, smaller sets are preferable, as they correspond to lower predictive uncertainty.

### D.3. LLM Prompt Template.

#### Prompt template

This is a text classification task.

You will get one example, then predict the most appropriate label.

Return only the label.

Example:

Text: <source\_text>

Label: <source\_label>

Text: <target\_text>

Label: